

EXPERIMENTAL STUDY OF THE TOW BUCKLING DEFECT. TOWARDS THE DETERMINATION OF A MULTI-FACTOR APPEARANCE CRITERION FOR THE FORMING PROCESS SIMULATION.

¹Pierre Ouagne, ¹Christophe Tephany, ¹Jean Gillibert, ²Damien Soulat

¹Laboratoire PRISME, MMH, Université Orléans, Orléans, France
pierre.ouagne@univ-orleans.fr, christophe.tephany@univ-orleans.fr, jean.gillibert@univ-orleans.fr,
²GEMTEX, ENSAIT Roubaix Roubaix, France
Damien.soulat@ensait.fr

Keywords: Woven fabric, Forming defect, Tow buckling, multi-factor appearance criterion

Abstract

During the manufacturing of composite complex shape parts, defects such as tow buckles characterised by out of plane elevation may appear. The parameters controlling the appearance and growth of the defect are not completely understood and need to be investigated. A device capable of reproducing tow buckles has been used to study the tow buckling phenomenon. Several techniques able to measure out of plane elevations have been particularly discussed to detect the appearance and evaluate continuously the growth of the tow buckle in relation to its size and shape. The fringe interferometry was chosen as it gives the best compromise between the size of the defect to measure and its resolution.

If the in-plane bending angle is the main criterion at the origin of the tow buckle appearance and growth, it is not the only one. This work shows that the fabric architecture such as the space between the tows perpendicular to the one showing the buckle is also crucial to control the buckle's appearance and growth.

1. Introduction

During the manufacturing process, defects may occur in composite parts. Potter et al. [1] have presented a list of defect states that may occur during the composite manufacturing processes. Some of the defects appearing during the first step of the RTM process (preforming stage) may have adverse impacts on the performance of composite parts and should be prevented [2, 3]. At the scale of the preform, denoted macroscale, it is possible to investigate if the preform shape is well obtained, if wrinkles appear, if there is non-homogeneity of the fibre density in tows, or if a discontinuity of the preform due to sliding of tows takes place [4-8]. At this scale, a lot of studies [9-15] have been published on the use of full field optical measurements of strains which provide an ideal instrument quantifying the strain levels in different deformation modes (tension, in-plane shear). At the scale of the tows, meso-scale, other defects may appear. Tow misalignment in the plane of the fabric, [1] or out-of-plane misalignment also called tow buckles [4,16,17], can be investigated. All these defects have a strong influence on the resin flow impregnation because they modify the in-plane and through-the thickness permeability components [18-22], and they impact the performance of the composite part.

By working on the forming process, Ouagne et al., Capelle et al. [16, 17] showed that the appearance of this defect depends on multiple criteria. They manage during their studies to prevent or limit the

buckles appearance by working on the reinforcement architecture and on the forming process parameters.

If some experimental work has already been carried out on the reduction or on the prevention of the buckles occurrence, all the parameters controlling the buckles appearance have not been yet identified with accuracy. By analogy with the wrinkling defect or pull-out defects which have been widely studied, this work proposes to study independently of the preforming process the tow or yarn buckling defect. Indeed, a lot of work has been devoted to study the relationship between the in-plane shear phenomenon and the appearance of the wrinkling defect mainly caused by the locking of warp and weft yarns [23-24]. During the forming process, the appearance of wrinkling is not only due to in-plane shear but also to the tension of the membrane and the bending stiffness. Several authors therefore decided to study independently of the process this defect by designing specific in-plane shear characterisation protocols using either the bias extension test or the picture frame test [1, 14, 25, 26]. Kirkwood et al. [27] also used the same approach to study independently of the process the yarn pull-out phenomenon by designing an especially dedicated set-up.

Non-destructive Evaluation (NDE) techniques have been employed to inspect and characterize composite structures [28]. Various NDE methods, such as the optical techniques of holography, electronic speckle-pattern interferometry, shearography and time-domain moiré interferometry, are used for thermoplastic or thermoset composites and are described by a number of authors [29-35]. These techniques provide wide-area qualitative imagery in the in- and out-of-plane displacement at the surface of a structure, and their effectiveness at inspecting structures of any significant thickness for buried defects is normally vastly reduced [28]. If the use of all these methods is well described for composite parts, the detection of defects at the scale of fabrics, before injection of resin, and associated to this preforming stage, has not really been studied.

In this paper an experimental device to reproduce the tow buckling phenomenon is used and is associated to moiré interferometry to quantify the out-of-plane defect.

2. Tow buckling defect: parameters controlling its appearance

During the forming of particular complex shapes such as tetrahedron or prism the tow buckle defect may appear. This defect appears in specific zones of the formed shapes as shown in Figure 1. On the tetrahedron, shape, the buckles appear on a localised zone converging to the top of the shape, and also on one of its edge [17]. As shown by Figure 1, the tow buckling defect is characterised by an elevation of tows out of the plane of the fabric. The height of the buckles has been reported on the same study to be as high as 2 mm for the considered flax woven fabric. The size of the buckles is not homogeneous on the buckle's zone. As the defect is localised and its size not constant along the buckle's zone, the preform is therefore not homogeneous. As a consequence, the formed shape cannot be accepted. This defect has been reported by several authors for different types of textile architectures and different natures of tows within fabrics. Potter et al [19] reported out of plane buckling of tows in a carbon woven fabrics. Beakou et al [35] reported and modelled the appearance of tape buckling during the robot lay-up of carbon prepreg. Ouagne et al [17, 36], Allaoui et al [37], showed that tow buckles appear in specific zones of complex shapes when flat based rectangular tows are used. The buckles were observed for flax based plain weave and twill weave fabrics and on interlock carbon fabric.

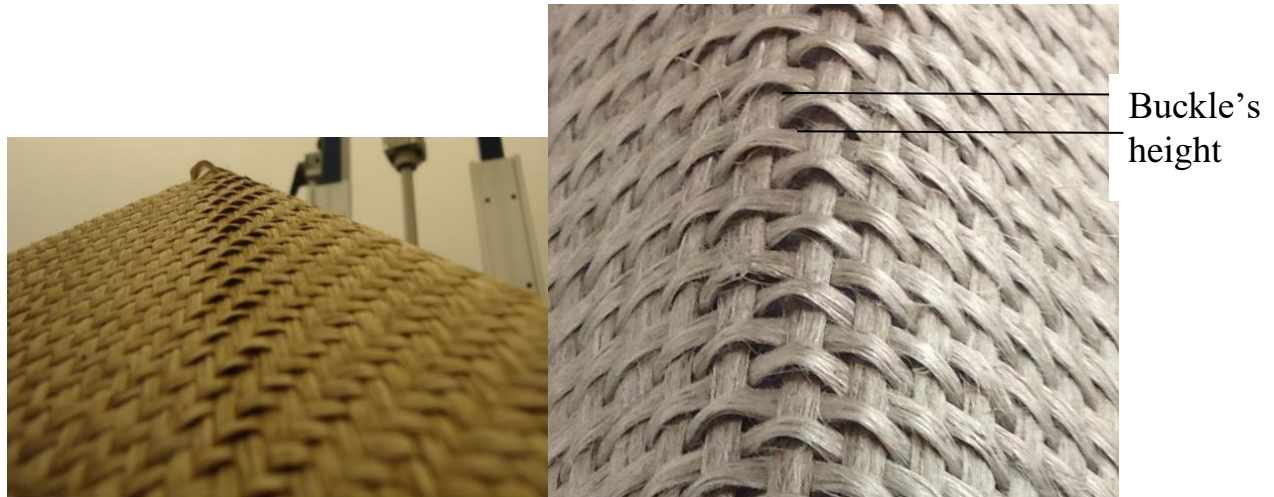


Figure 1 : Tow buckling phenomenon on the face and on one edge of a tetrahedron shape

As described in the previous paragraph, the tow buckling defect may appear on laid up prepreg tapes as well as on tows within a fabric. Beakou et al [35] modelled the appearance of defects analogous to the ones shown in Figure 1 in the frame of prepreg tape lay-up. However, the appearance of tow buckles in woven fabrics is more complex. In the first studies reporting the appearance of the tow buckling defect during the forming process, the main mechanism without which the tow buckling defect cannot appear has been identified for different carbon, glass and flax flat tow based woven fabrics [17, 36, 37]. This mechanism is the bending in their plane of flat tows imposed by the geometry of the complex shape. As this mechanism cannot be or can only be partially accommodated by the tow, another mechanism consisting in deforming the tow out of its plane takes place and a buckle as shown in Figure 1 appears. The measurements performed on a face of a tetrahedron where tow buckling appears show that globally, the bending angles remain similar all along the buckling zone with lower values (more severe bending) towards the top of the shape. This bending angle quasi-continuity means that the displacements of the tows exhibiting the buckles are almost similar and symmetrical against the curvature point line shown in Figure 2.

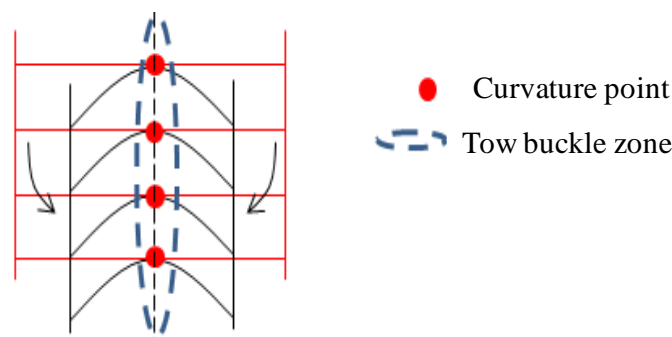


Figure 2: Principle of the tow in-plane bending during the forming process of a tetrahedron shape

However, the in-plane bending of the tow is not the only parameter influencing the appearance of the tow buckles. The tensile deformation of the tows perpendicular to the ones exhibiting the buckles was shown to be an important parameter to delay and reduce the magnitude of the buckles size. Ouagne et al [38] showed that the tensile strains of the tows, situated in the buckle's zone, are the highest of the ones recorded on the different areas of the shape. Particularly, the deformations of the tows passing by the top of the tetrahedron shape are the highest ones, and the magnitude of the tensile deformation decreases as a function of the distance from this tow. As the buckles are situated in high tensile strain

zones [39], blank holders to reduce the tension of the tows perpendicular to the ones showing the buckles were designed [8]. That study showed that it was possible to reduce the size of the buckles and to delay their appearance by reducing the tensile strains in the tows perpendicular to the ones showing the buckles. It is important to note that the deformation of the tows passing by the top of the tetrahedron depends on the architecture of the fabric. As an example, an un-balanced fabric does not show equivalent tensile strains in these tows for both warp and weft directions, and the magnitude of the buckle's size may be affected.

Ouagne et al [7] showed that the appearance of buckles could be prevented on the face of the tetrahedron shape they studied by reducing the space between flat tows perpendicular to the ones exhibiting the buckles. In these conditions, the tow does not have a wide enough space to allow the development of a buckle. In the same work the authors showed that a hopsack fabric manufactured from cylindrical yarns did not exhibit any tow buckles. This means that the meso-architecture of the fabric is also very important and should be an important point of study.

The previous paragraph therefore demonstrates that the appearance of tow buckles depends on multiple factors. As a consequence, the design of a device capable of reproducing independently of the forming process this defect should take into account all these parameters.

3. Materials and methods

3.1 Presentation of the buckling device

The experimental device presented in Figure 3 is able to apply tensions in two directions. A first fixed axis applies a tension to tows originally perpendicular to the ones which are supposed to show buckles (Figure 4a). On the tetrahedron preform (Figure 2), these are the vertical tows. The second axis is constituted of two mobile jaws that perform a circular translation. The circular translation movement is conferred in each side of the mobile axis by two pivoting axis as shown in Figure 4c. Those elements have been designed so that to prevent any out of plane bending of these two axes when tension loads are applied. Two parallel bars have been placed in this goal. The reinforcement is held in four zones between two thin steel plates (2 mm thick) as it is the case for the biaxial tension tests [29] placed within the jaws. Pressure screws impose a load on plates placed within the jaws. The jaws can slide on their support (fixed or mobile) and their movement is conferred by filet rods for each direction (Figure 4d). The loads can be measured by an in house made train gage based sensor (Figure 4d). The sensors measurement range is contained between 0 and 1kN.

The displacement of the circular translation jaws is imposed by two filet rods associated to springs to anneal the unwanted slack movements (Figure 4b).

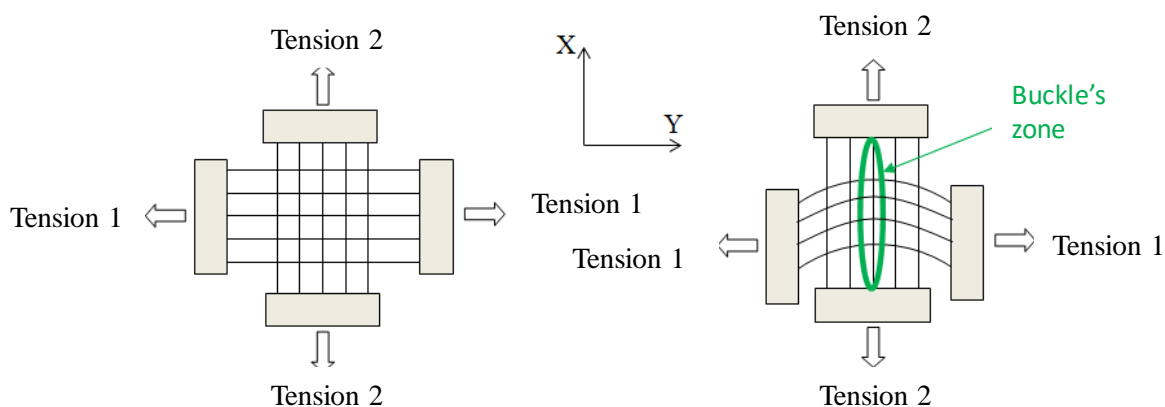


Figure 3 : Principle of the tow buckling device

3.2 Material

The reinforcement used in this study is a plain weave fabric manufactured by Groupe Depestele (France). The reinforcement is not balanced and is constituted of continuous rectangular untwisted yarns. The characteristics of the plain weave reinforcement are presented in Table 1.

Table 1: Plain weave fabric characteristics

Reinforcement composition	100% flax	
Manufactured by	Groupe Depestele (France)	
Reinforcement structure	Plain weave	
Yarn structure	Flat yarns	
Linear mass of yarns [tex]	Warp : 468.2 ± 34.78	Weft : 537.7 ± 44.36
Fabric areal weight [g/m ²]	262±15	
Average width of yarns [mm]	Warp : 2.12 ± 0.35	Weft : 2.46 ± 0.28
Average space between yarns	Warp 0.26 ± 0.01	Weft 1.59 ± 0.09

4. Results and discussion

4.1 Profile of the fabric and of the tow buckles

On a first extent, a piece of the plain weave fabric is placed on the device with an orientation 0°. The warp tows are the ones which are submitted to in-plane bending. The square periodic profile of elevation of a tow in the plain weave fabric is shown in Figure 4a at the initial stage. The square profile is globally reproduced even if measurement artefacts are observed. Figure 4b shows the profile of altitude of the same zone at the final state of the test. This one differs from the idealised profile of tow buckles observed on one edge of a tetrahedron shape (Figure 5 b). The idealised profile of Figure 5b shows that the buckles rise continuously on one side of their width.

4.2 Profile of the buckles at the initial and at the final states

The profile of altitude along the X-axis has been recorded by the device for the studied reinforcement (Figure 4). In Figure 4, the profile of altitude is presented at the initial state (bending angle 0°) and the final state (bending angle of 42°). No tensile loads were applied in the direction perpendicular to the direction of the tow supposed to exhibit buckles. A clear variation of altitude can be observed between the initial and the final state, with elevations growing from about 0.4 mm up to 1.6 mm.

At the initial state, a square peak profile can be observed. Two different mean altitudes can be observed. These two altitudes correspond to the two directions of the tows within the fabric. Between two following plateaus of higher elevation, lower altitudes can be observed. These lower altitudes are due to the fact that the tow perpendicular to the one exhibiting the buckles passes below it. On the measurements presented in Figure 4a, the tows showing the higher plateaus are situated at an average elevations of 0.39 ± 0.03 mm above the medium plane which is the reference elevation value 0°. The tows perpendicular to these ones are situated below the medium plane at a value of -0.11 ± 0.04 mm.

At the final stage, Figure 4b shows that the profile of the peak changes between the initial and the final state and shows the spatial evolution of the tows. The peaks are characterized by a progressive rise of the elevation up to a maximum. After the maximum elevation point, a brutal drop of altitude is observed like in the buckle's profile presented on Figure 5b for the formed tetrahedron shape. Before the peak, a compression phenomenon takes place. The tow exhibiting the buckle imposes a compression load on one of its side to the perpendicular tow as schematically represented in Figure 6. On one side of the tow the point A presents a positive elevation. At the end of the buckle formation,

the point A is situated at a maximum elevation. In the other side of the tow (point B) a negative elevation due to a compression of the tow on the perpendicular tow passing underneath it takes place. This phenomenon is the inverse consequence of the rise of the buckle. During the rotation of the tow around the Z-axis, another rotation around the Y-axis takes place. It is interesting to note that the axis of rotation around the Y axis is not situated in the middle of the tow. The width percentage of the tow in compression measured on the profile of the buckle (Figure 4b) is of about 25%. One can also observe that the tows perpendicular to the ones exhibiting the buckles do not show a plateau anymore. They are characterised by a chevron profile which means that the lower elevation value is situated in a lower position that at the initial state: -0.4 ± 0.2 mm. The highest point of these tows is also situated at a lower elevation: -0.26 ± 0.04 mm. At the final state, one can also observe that the positions of the peaks are slightly translated in the x-direction. This is due to the displacement imposed to the fabric (and therefore to the tows) during the test.

At the initial state, some very important decreases of altitudes are observed after the peaks (Figure 4 a). These phenomena are probably the result of measurement artefacts due to the fact that the video projector light does not penetrate correctly in this particular zone and therefore, the altitude measurement is not correct.

Globally, the change of elevation between the maximum initial and final values of the tow exhibiting the buckles is within the range 1-1.2 mm. These results can be compared to measurements carried out on the tetrahedron shape [7] with the same fabric. Globally a good correspondence can be observed between the results presented in this work and the ones presented in [7] for low blank holder pressure on the face of the tetrahedron where values of about 1.1 ± 0.1 mm of elevation were recorded.

All the previous observations therefore indicate that the device is able to reproduce buckles with similar characteristics than the ones observed on the formed shape (Figure 5) and also that the interferometry technique is completely adapted for the measurement of the buckle's elevation.

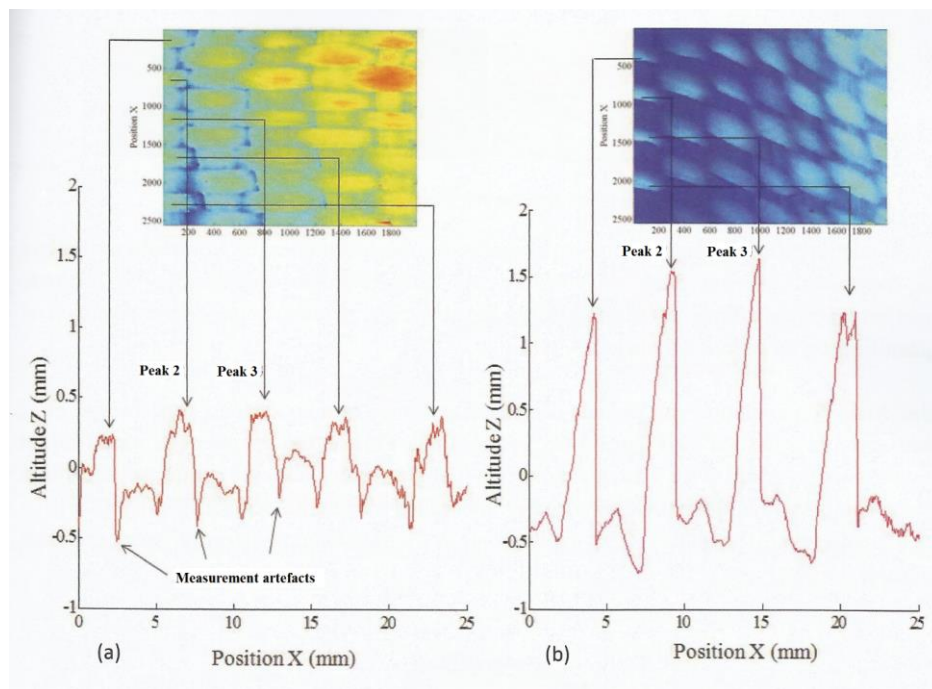


Figure 4 : Elevation profile for the plain weave fabric: (a) initial state; (b) final state

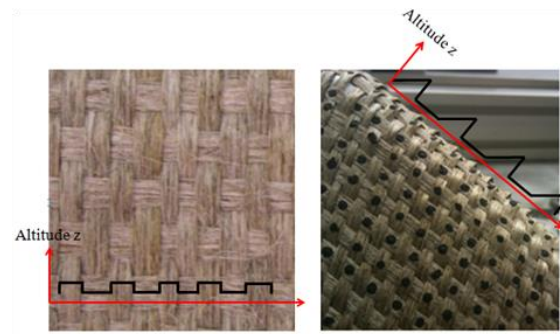


Figure 5: Profile of altitude of a plain weave fabric (a); tow buckle's profile(b)

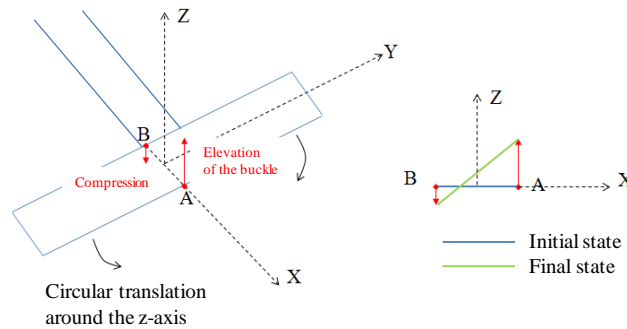


Figure 6: Schematic diagram of the tow buckling appearance and growth

4.3 Evolution of the buckle's profile as a function of the bending angle

Figure 7 shows the profile of altitude of tows 2 and 3 as defined in Figure 4 as a function of the in-plane bending angle from the initial to the final state of the test. Each curve of the graph represents a different bending angle with an evolution of 1°. In Figure 7 a and c, the profile evolution is presented for bending angle situated within the 0-28° range. A progressive modification of the profile can be observed. However, up to the bending angle of 28°, the profile shows a quick rise of altitude followed by a plateau and a progressive drop of altitude. The drop of altitude becomes steeper for bending angles values of about 28°. If the profile remains globally similar, a rise of the plateau from an angle of about 20° is observed. The altitude changes from a value of about 0.4 mm to a value of about 0.75 mm. A difference of 85% is observed.

Above 28° (Figures 7b and d), the modification of the profile becomes more significant. The plateau situated after the initial rise of altitude progressively disappears and is replaced by a continuous rise of elevation up to the top of the buckle followed by a sudden drop. On the last bending angle variations, the profile does not almost vary anymore. One can therefore suppose that the buckle is completely formed and its growth stopped. This phenomenon takes place for an in-plane bending angle of about 40°. Figure 8 summarises the evolution of the elevation as a function of the bending angle.

Comparisons with bending angles measured on the face of a tetrahedron presenting tow buckles [7] with similar elevations to the ones measured in this work indicate that the bending angles are situated in the range 35-42° for low blank-holder pressures. Once again, the measurements performed with the device are in good agreements with measurements performed at the end of the forming process with similar conditions.

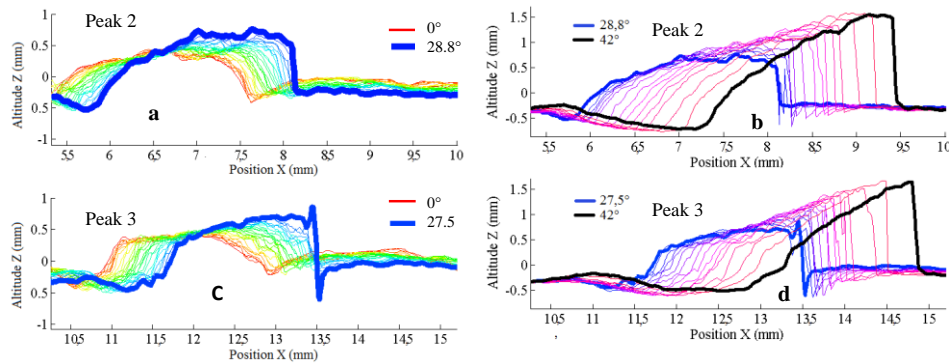


Figure 7 : Profile evolution of the tow exhibiting the buckle for increasing in-plane bending angles

The elevation of the buckles at the final state is of about 1.6 ± 0.2 mm above the medium plane of the fabric. This value should then be compared to the width of the tow (2.12 mm). This means that the tow is capable to reach an elevation corresponding to about 75% of its width. The other part is situated below the medium plane and represents the part that imposes a compression load on the perpendicular tow.

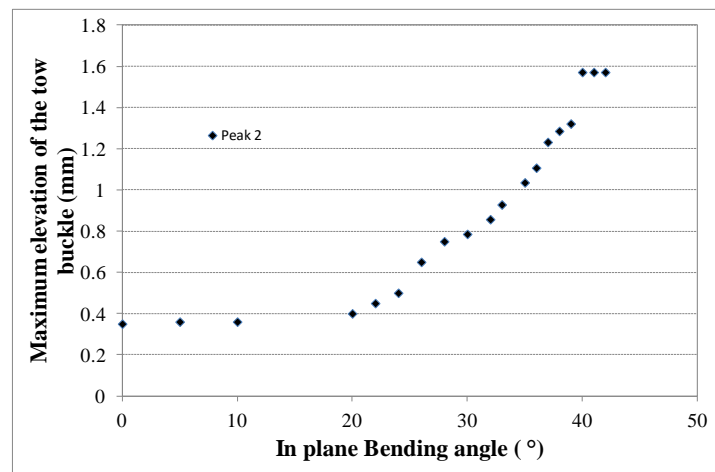


Figure 8: Evolution of the maximum elevation of the tow buckle as a function of the in plane bending angle.

5. Conclusions

With the view to investigate the tow buckling defect independently of the process, a device capable to reproduce the defect was designed and associated to a specific instrumentation. Particularly, structure light interferometry was chosen to measure the elevation of the tows exhibiting the buckling defect all along its growth. The device and its instrumentation were validated in this work and a preliminary study was performed to investigate the origin of the tow buckle's appearance and its growth cinematic. It was shown that the in-plane bending of the tow is a key parameter controlling the appearance of the defect and its growth up to a maximum elevation above the medium plane of the fabric that is controlled by the geometry of the tow but also by its respective stiffnesses (bending and compression). This parameter can probably be considered as a preliminary criterion that conditions the appearance and the growth of the tow buckling defect. The growth cinematic of the buckle's appearance consisting on a double simultaneous rotation of the tow exhibiting the buckle around the Z and the Y axis was established. Due to the rotation of the tow around the Y-axis, one side of the tow imposes a compression load to the perpendicular tow. As a consequence, the profile of this tow changes from a square profile to chevron profile.

This work even if of a preliminary nature establishes a criterion conditioning the appearance and

describes the growth cinematic of the tow buckling defect. This work also establishes the basis necessary for a wider study of all the parameters that may influence the appearance and growth of the tow buckling defect by using the device and its specific instrumentation designed and exposed in this work.

References

- [1] Wang P, Hamila N and Boisse P. Thermoforming simulation of multilayer composites with continuous fibres and thermoplastic matrix. *Composites Part B* 2013; 52: 127-136
- [2] Liang B., Hamila N, Peillon M., Boisse P. Analysis of thermoplastic prepreg bending stiffness during manufacturing and of its influence on wrinkling simulations. *Composites: Part A* 67 (2014) 111–122
- [3] Gereke T., Döbrich O., Hübner M., Cherif C. Experimental and computational composite textile reinforcement forming: A review. *Composites: Part A* 46 (2013) 1–10.
- [4] Chen S., Endruweit A., Harper L.T., Warrior N.A. Inter-ply stitching optimisation of highly drapeable multi-ply preforms. *Composites: Part A* 71 (2015) 144–156.
- [5] Allaoui S., Cellard C., Hivet G. Effect of inter-ply sliding on the quality of multilayer interlock dry fabric Preforms. *Composites: Part A* 68 (2015) 336–345.
- [6] Smerdova, O., Sutcliffe, M.P.F., Multiscale Tool-Fabric contact observation and analysis for composite fabric forming, *Composites Part A: Applied Science and Manufacturing*, Volume 73, June 2015, Pages 116-124
- [7] Ouagne P, Soulat D, Moothoo J, Capelle E and Gueret S. Complex shape forming of a flax woven fabric; analysis of the tow buckling and misalignment defect. *Composites Part A* 2013; 51: 1–10.
- [8] Capelle E, Ouagne P, Soulat D and Duriatti D. Complex shape forming of flax woven fabrics: Design of specific blank-holder shapes to prevent defects. *Composites Part B* 2014; 62: 29–36.
- [9] Pazmino J., Mathieu S., Carvelli V., Boisse P., Lomov S.V. Numerical modelling of forming of a non-crimp 3D orthogonal weave E-glass composite reinforcement. *Composites: Part A* 72 (2015) 207–218
- [10] Dufour C, Wang P, Boussu F and Soulat D. Experimental Investigation About Stamping Behaviour of 3D Warp Interlock Composite Preforms. *Applied Composite Material* 2014; 21(5): 725-738.
- [11] Peng X, Guo Z, Diu T and Yu WR. A simple anisotropic hyperelastic constitutive model for textile fabrics with application to forming simulation. *Composites Part B* 2013; 52: 275–281.
- [12] Hamila N., Boisse P. Locking in simulation of composite reinforcement deformations. Analysis and treatment. *Composites: Part A* 53 (2013) 109–117
- [13] Bloom LD, Wang J, Potter KD. Damage progression and defect sensitivity: an experimental study of representative wrinkles in tension. *Composites: Part B* 2013;45:449–58.
- [14] Lee J, Hong S, Yu W, Kang T. The effect of blank holder force on the stamp forming behavior of non-crimp fabric with a chain stitch. *Compos Sci Technol* 2007;67:357–66.
- [15] Lin H, Wang L, Long AC, Clifford MJ, Harrison P. Predictive modelling for optimization of textile composite forming. *Compos Sci Technol* 2007;67:3242–52.
- [16] Boisse P, Hamila N, Vidal-Sallé E and Dumont F. Simulation of wrinkling during textile composite reinforcement forming. Influence of tensile, in-plane shear and bending stiffnesses. *Compos Sci Technol* 2011; 71(5): 683-692
- [17] Ouagne P, Soulat D, Hivet G, Allaoui S, Duriatti D. Analysis of defects during the preforming of a woven flax. *Adv Compos Lett* 2011;20:105–8.
- [18] Gatouillat S, Bareggi A, Vidal-Sallé E and Boisse P. Meso modelling for composite preform shaping. Simulation of the loss of cohesion of the woven fibre network. *Composites Part A* 2013; 54: 135–144.
- [19] Potter K, Khan B, Wisnom M, Bell T, Stevens J. Variability, fibre waviness and misalignment in the determination of the properties of composite materials and structures. *Composites: Part A* 2008;39:1343–54.
- [20] Walther J, Simacek P, Advani SG. The effect of fabric and fiber tow shear on dual scale flow and fiber bundle saturation during liquid molding of textile composites. *Int J Mater Form* 2012;5:83–97.
- [21] Vernet, N., Ruiz, E., Advani, S. et al. Experimental Determination of the Permeability of Engineering Textiles: Benchmark II. *Composites Part A: Applied Science and Manufacturing*, Volume 61, June 2014, Pages 172-184
- [22] Ouagne P, Bréard J. Continuous transverse permeability of fibrous media. *Composites: Part A* 2010;41:22–8.
- [23] Ouagne P, Ouahbi T, Park C-H, Bréard J, Saouab A. Continuous measurement of fiber reinforcement permeability in the thickness direction: experimental technique and validation. *Composites: Part B* 2012;45:609–18.

- [24] Van Den Brouck B., Hamila N., Middendorf P., Lomov S.V., Boisse P., Verpoest I. Determination of the mechanical properties of textile-reinforced composites taking into account textile forming parameters *Int J Mater Form* (2010) 3 (Suppl 2):S1351–S1361
- [25] Hamila N., Boisse P. Simulations of textile composite reinforcement draping using a new semi-discrete three node finite element. *Composites: Part B* 39 (2008) 999–1010
- [26] Boisse P, Zouari B, Daniel JL. Importance of in-plane shear rigidity in finite element analyses of woven fabric composite preforming. *Composites A* 2006;37(12):2201–12.
- [27] Cao J., et al. Characterization of mechanical behavior of woven fabrics: Experimental methods and benchmark results. *Composites: Part A* 39 (2008) 1037–1053
- [28] Hivet G., Boisse P. Consistent mesoscopic mechanical behaviour model for woven composite reinforcements in biaxial tension. *Composites: Part B* 39 (2008) 345–361
- [29] Gasser A., Boisse P, Hanklar S. Mechanical behaviour of dry fabric reinforcements. 3D simulations versus biaxial tests. *Computational Materials Science* 17 (2000) 7±20
- [30] de Bilbao E, Soulat G, Launay D, Hivet J, Gasser A. Experimental study of bending behaviour of reinforcements. *Exp Mech* 2010;50(3):333–51.
- [31] Allaoui S, Hivet G, Wendling A, Ouagne Soulat P. Influence of the dry woven fabrics meso-structure on fabric/fabric contact behavior. *J Compos Mater* 2012;46(6):627–39.
- [32] Ten Thije RHW, Akkerman R, Ubbink M, et al. A lubrication approach to friction in thermoplastic composites forming processes. *Compos Part A: Appl Sci Manufac* 2011; 42: 950–960.
- [33] Walid Najjar W., Pupin C., Legrand X., Boude S., Soulat D., Dal Santo P. Analysis of frictional behavior of carbon dry woven reinforcement. *Journal of Reinforced Plastics and Composites*, June 2014; vol. 33, 11: pp. 1037-1047
- [34] Arbter R, Beraud JM, Binetruy C, Bizet L, Bréard J, Comas-Cardona S, et al. Experimental determination of the permeability of textiles: a benchmark exercise. *Composites Part A* 2011;42:1157–68.
- [35] Beakou A, Cano M., Le Cam J. B., Verney V. Modelling slit tape buckling during automated prepreg manufacturing: A local approach. *Composite Structures*, Volume 93, Issue 10, September 2011, Pages 2628-2635.
- [36] Ouagne P., Soulat D., Allaoui, S., Hivet G. Mechanical properties and forming possibilities of a new generation of flax woven fabrics. *Proceeding of the 10th international conference on textile Composite (Texcomp)*. 26-28 Octobre 2010, Lille.
- [37] Allaoui S., Hivet G., Soulat D., Wendling A., Ouagne P., Chatel S.. Experimental preforming of highly double curved shapes with a case corner using an interlock reinforcement. *International Journal of Material Forming*. Volume 7, Issue 2, June 2014, pp.155-165.